Chromosome detachment from the nuclear envelope is required for genomic stability in closed mitosis

Rey-Huei Chen*
Institute of Molecular Biology, Academia Sinica, Taipei 11529, Taiwan

ABSTRACT **Mitosis in metazoans involves detachment of chromosomes from the nuclear envelope (NE) and NE breakdown, whereas yeasts maintain the nuclear structure throughout mitosis. It remains unknown how chromosome attachment to the NE might affect chromosome movement in yeast. By using a rapamycin-induced dimerization system to tether a specific locus of the chromosome to the NE, I found that the tethering delays the separation and causes missegregation of the region distal to the tethered site. The phenotypes are exacerbated by mutations in kinetochore components and Aurora B kinase Ipl1. The chromosome region proximal to the centromere is less affected by the tether, but it exhibits excessive oscillation before segregation. Furthermore, the tether impacts full extension of the mitotic spindle, causing abrupt shrinkage or bending of the spindle in shortened anaphase. The study supports detachment of chromosomes from the NE being required for faithful chromosome segregation in yeast and segregation of tethered chromosomes being dependent on a fully functional mitotic apparatus.**

Monitoring Editor
Kerry S. Bloom
University of North Carolina

Received: Feb 12, 2019
Revised: Apr 18, 2019
Accepted: Apr 18, 2019

INTRODUCTION

The eukaryotic genome is organized in the nucleus partly through multiple associations of the chromosome with the nuclear envelope (NE) at interphase. In metazoans, the chromosome–NE association is disrupted upon mitotic entry marked by chromosome condensation, NE breakdown (NEBD), and mitotic spindle formation (Champion *et al.*, 2017). NEBD permits capture of chromosomes by the mitotic spindle, which is enucleated from the centrosome located in the cytoplasm. NEBD and detachment of chromosomes are mediated by phosphorylation of inner nuclear membrane and chromosomal proteins by multiple mitotic kinases (Heald and McKeon, 1990; Foisner and Gerace, 1993; Hirano *et al.*, 2005, 2009; Nichols *et al.*, 2006; Molitor and Traktman, 2014). Perturbation of the phosphorylation events affects chromosome congression to the metaphase plate and subsequent chromosome segregation (Tseng and Chen, 2011; Molitor and Traktman, 2014). By linking histone H2B to an endoplasmic reticulum membrane protein to sustain membrane–chromatin association, one research group has recently shown that detachment of chromatin from the NE in early mitosis is required for proper chromosome segregation (Champion *et al.*, 2019).

Unlike metazoans, yeast cells maintain an intact nuclear structure during nuclear division, so-called closed mitosis. The yeast spindle pole body (SPB), equivalent to the centrosome in animal cells, is embedded in the NE and thus enucleates spindle microtubules in the nucleus without a need for NEBD. Interphase yeast chromosomes are associated with the NE at telomeres through multiple telomere-associated proteins, including the DNA-binding protein Rap1, the Ku70 and Ku80 heterodimer, and the silencing proteins of the Sir complex (Laroche *et al.*, 1998; Hediger *et al.*, 2002; Taddei and Gasser, 2004). NE attachment involves inner nuclear membrane proteins Esc1 in budding yeast (Taddei *et al.*, 2004) and the Bqt3-Bqt4 complex in fission yeast (Chikashige *et al.*, 2009). Telomeres are transiently released from the NE during mitosis (Hediger *et al.*, 2002; Fujita *et al.*, 2012), accompanied

This article was published online ahead of print in MBoC in Press (http://www.molbiolcell.org/cgi/doi/10.1091/mbc.E19-02-0098) on April 24, 2019.

The author declares no conflict of interest.

*Address correspondence to: Rey-Huei Chen (reyhuei@gate.sinica.edu.tw).

Abbreviations used: Chr, chromosome; GFP, green fluorescent protein; INM, inner nuclear membrane; NE, nuclear envelope; NEBD, nuclear envelope breakdown; SPB, spindle pole body.

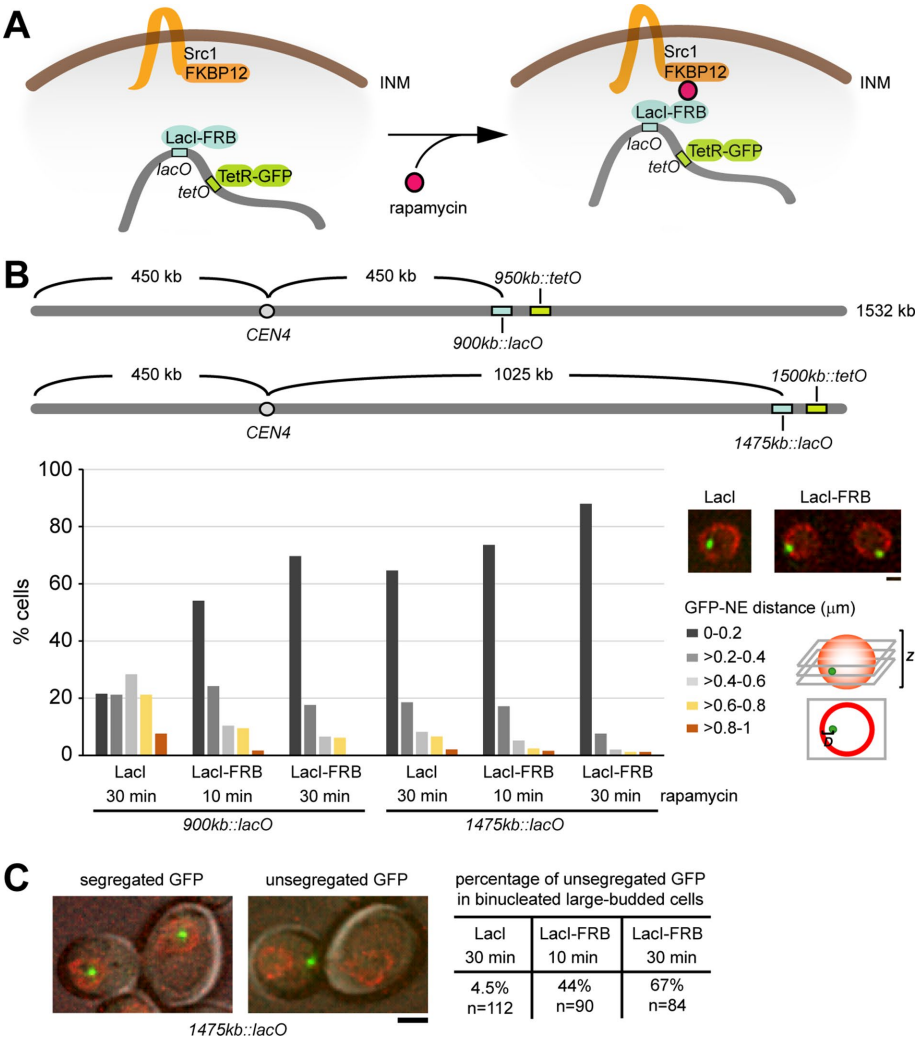

FIGURE 1: Tethering of the chromosome to the NE. (A) Design of the inducible chromosome-tethering system. INM, inner nuclear membrane. (B) The diagram shows the insertion sites of *lacO* and *tetO* repeats. The distance between tetR-GFP dot to the NE marked by Nup2-mCherry was measured (230–250 cells for each sample) in cells treated with rapamycin for 10 or 30 min as indicated. Representative images of a single focal plane containing the GFP dot near the center of the nucleus are shown. Scale bar: 1 μm. (C) Quantification of unsegregated tetR-GFP dot in binucleated large-budded cells treated with rapamycin for 10 or 30 min. Images are z-stacks processed by deconvolution and maximum-intensity projection. Scale bar: 2 μm.

RESULTS AND DISCUSSION

To tether a specific chromosome locus to the NE, I combined the chromosomal *lacO*/LacI–green fluorescent protein (GFP) system and the rapamycin-inducible anchor-away technique. Rapamycin induces high-affinity association between the FRB domain of mTOR and the rapamycin acceptor FKBP12, bridging proteins fused separately to these domains (Haruki *et al.*, 2008). I generated the NE anchor by tagging the integral nuclear membrane protein Src1 with two copies of FKBP12 and expressed LacI-FRB fusion protein as the target. LacI-FRB binds to the *lacO* array integrated at a specific chromosomal locus and directs the locus to the NE through the rapamycin-induced dimerization between LacI-FRB and Src1-2xFKBP12 (Figure 1A). This system permits conditional chromosome tethering to the NE to minimize any adverse effect from constitutive tethering. To monitor chromosome dynamics, I also integrated a *tetO* repeat sequence at a desired locus and expressed tetR-GFP for visualization.

I examined the efficiency of tethering at two loci of chromosome IV (ChrIV) by inserting the *lacO* repeats at either 900 kb in the middle of the right arm or 1475 kb near the right telomere, along with *tetO* repeats at 950 and 1500 kb, respectively (Figure 1B). For *900kb::lacO* cells expressing LacI as control, the tetR-GFP dot resided at various distances from the NE marked by Nup2-mCherry, which was expected for a nontethered chromosome arm region (Figure 1B). The GFP dot was enriched at the nuclear periphery in cells expressing LacI-FRB after the addition of rapamycin for 10 min, which was further enhanced after 30 min (Figure 1B). For *1475kb::lacO*, the tetR-GFP dot was located near the nuclear periphery in >60% of LacI cells, consistent with telomere–NE association (Figure 1B). In LacI-FRB cells, the perinuclear association of the GFP signal was gradually increased after adding rapamycin for 10–30 min (Figure 1B). Thus, rapamycin quickly induces the tethering of both the arm and the end of chromosomes to the NE.

In large-budded cells that have divided the nucleus, >90% of LacI cells contained a tetR-GFP dot in both nuclei (Figure 1C). However, a single GFP focus located between the divided nuclei or associated with one of the nuclei was found in 44% of LacI-FRB cells after rapamycin treatment for 10 min, and the fraction increased to 67% after 30 min (Figure 1C). This result suggests that tethering to the NE through Src1 perturbs chromosome segregation.

I next examined the effect of NE tethering on the dynamic movement of ChrIV, the second-largest chromosome of ~1532 kb in budding yeast. I reasoned that the effect might be more pronounced for large chromosomes, which take longer to segregate than small ones. The largest chromosome, ChrXII, was not used, because its repetitive rDNA sequence and heterogeneity in length could complicate the analysis. I monitored chromosome dynamics in mitosis

by a partial release of Rap1 and Sir proteins from telomeres in budding yeast (Laroche *et al.*, 2000) and phosphorylation of Rap1 in fission yeast (Fujita *et al.*, 2012). The transient detachment from the NE, partly as a result of Rap1 phosphorylation, is required for faithful chromosome segregation in fission yeast (Fujita *et al.*, 2012). Forced anchoring of telomeres to the inner nuclear membrane perturbs anaphase progression and generates chromosome bridges (Fujita *et al.*, 2012).

Previous chromosome–NE tethering systems either affect all chromosomes in mammalian cells (Champion *et al.*, 2019) or anchor all telomeres in fission yeast (Fujita *et al.*, 2012). As such, they did not provide the spatiotemporal resolution to determine how the persistent chromosome–NE association affects the dynamics of individual chromosomes. In this study, I designed a strategy to tether a specific chromosome locus to the NE and analyze its effect on the chromosome and spindle dynamics in budding yeast.

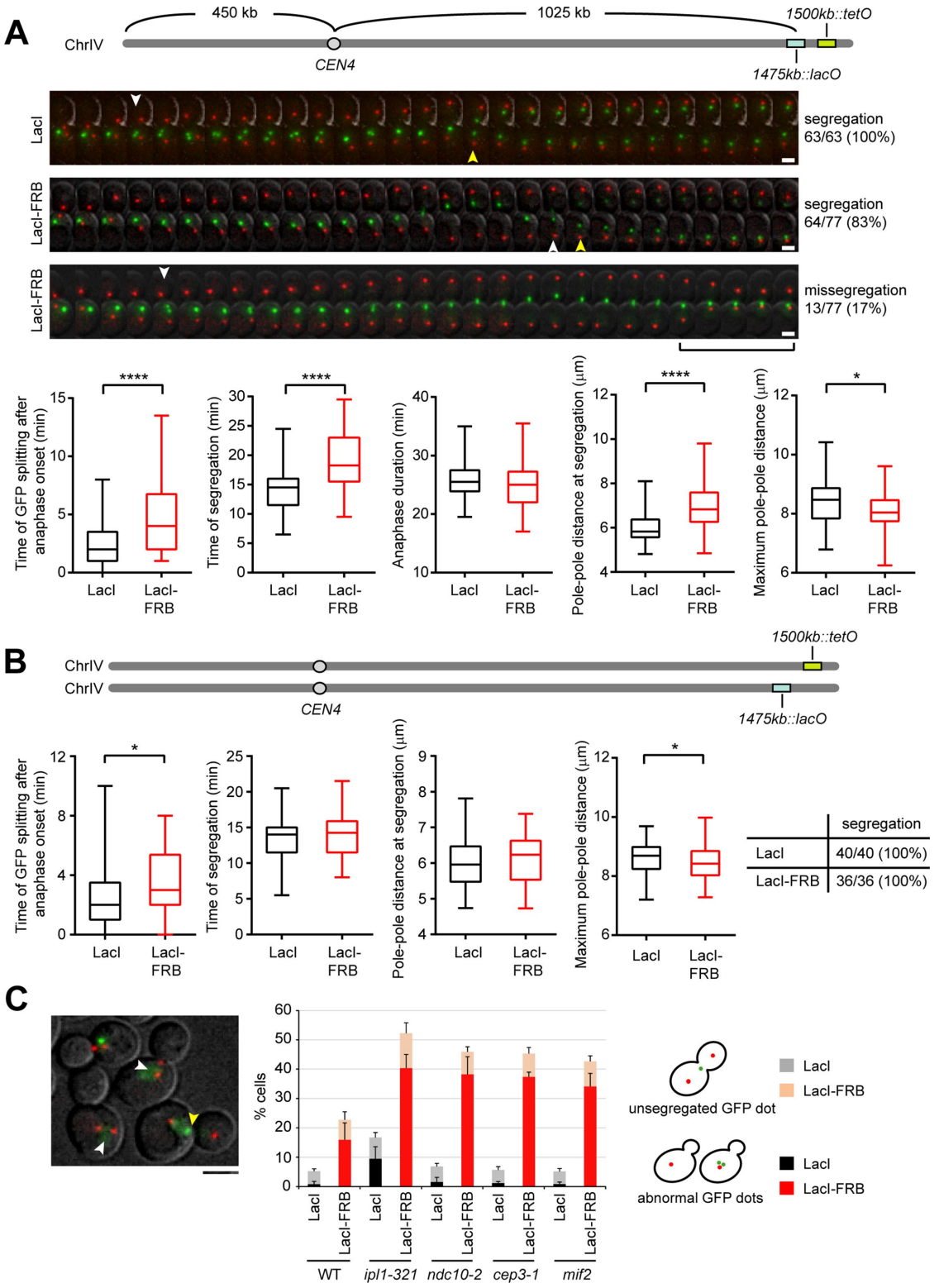

FIGURE 2: Effect of chromosome–NE tethering on the segregation of the distal region. (A) Time-lapse images of cells with *lacO* and *tetO* repeats inserted in ChrIV at 1475 and 1500 kb, respectively. Representative cells expressing LacI or LacI-FRB are shown. SPBs are marked by Spc42-mCherry. Maximum-intensity projection images with 1-min intervals are shown (see also Supplemental Video 1). White and yellow arrowheads indicate sister chromatid splitting and segregation, respectively. Bracket indicates abrupt migration of SPBs toward the bud neck. Scale bar: 2 μm. Measurements from the time series are plotted. The box covers the first to the third quartile; the horizontal line in the box represents the median; and the whiskers indicate the minimum and maximum. Two-tailed unpaired Student's *t* test, ****, $p < 0.0001$; *, $p < 0.05$. (B) Effect of chromosome tethering in *trans*. *lacO* and *tetO* repeats were separately inserted in homologous ChrIV of diploid cells. Measurements from time series are plotted, and the fraction of cells that

by time-lapse fluorescence microscopy. The onset of anaphase was marked when the distance between the SPBs labeled by Spc42-mCherry began to increase. In *1475kb::lacO* cells expressing LacI, the tetR-GFP dot split into two on average 2.65 min after anaphase onset at 27°C (Figure 2A), indicative of sister cohesion loss. Segregation of this region, as defined by separation of the GFP dots for >2 μm, occurred on average 14.06 min into anaphase, with one GFP dot moving into the bud (Figure 2A). All control cells examined (n = 63) successfully segregated the GFP dots by the end of anaphase, when the pole–pole distance started to shorten, with an average anaphase duration of 25.77 min (Figure 2A).

For cells expressing LacI-FRB to tether ChrIV at 1475 kb, 83% of the cells (n = 77) segregated the GFP dot, while their times of splitting and segregation were more variable and significantly longer than in LacI control cells, with an average of 4.89 and 19.09 min for splitting and segregation, respectively (Figure 2A). Notably, the GFP dot often split briefly and then reassociated until segregation, indicating that sister cohesion remained. This is consistent with a previous finding that perinuclear attachment imposes topological constraint for the resolution of intertwined DNA by topoisomerase II (Titos *et al.*, 2014). In addition, the GFP dot frequently oscillated between mother and bud before segregation, rather than moving one GFP dot from mother to bud, as in the control (Figure 2A). The GFP signal sometimes separated into two dots of different intensity (Figure 2A, top LacI-FRB panel), indicative of unequal segregation of *tetO* repeats. In 17% of the LacI-FRB cells, the GFP dot split briefly and then reassociated without segregation (Figure 2A, bottom LacI-FRB panel). In most of these cells (12 out of 13), the GFP dot moved to and stayed near the bud neck, while anaphase ended with SPBs moving quickly toward each other (Figure 2A, bottom LacI-FRB panel). The interpolar distance at the time of segregation was longer in cells carrying a tethered chromosome compared with the control, consistent with a delay in segregation. The maximum pole–pole distance on average was slightly shorter in cells with the tethered chromosome than in the control, suggesting that the tether prevents full extension of the mitotic spindle. These results show that tethering even a single chromosome locus to the NE can counteract the pulling force of the spindle and affect dynamic movement and segregation of the chromosome region distal to the tether.

I next asked whether tethering to the NE might affect chromosome dynamics in *trans* by using diploid cells carrying *lacO* and *tetO* inserts in separate ChrIV homologues at 1475 and 1500 kb, respectively (Figure 2B). Time-lapse microscopy showed that all LacI and LacI-FRB cells successfully segregated the tetR-GFP signal during anaphase with similar segregation time and pole–pole distance at segregation (Figure 2B). Therefore, the chromosome tether did not perturb chromosome segregation in *trans*, even though the tether still prevented full extension of the spindle (Figure 2B). The tether in *trans* caused a delay in the splitting of the GFP dot, which could be due to delayed sister resolution from an unknown connection between homologues or telomere clustering.

The pulling force from the mitotic spindle might overcome the chromosome tether and segregate the sister chromatids, albeit with a delay. I thus asked whether the segregation defect of the tethered chromosome might be enhanced by mutations that compromise the mitotic force. I examined temperature-sensitive mutants of the Aurora B kinase Ipl1, which is important for bipolar attachment of kinetochores to spindle microtubules (Stern, 2002), and three kinetochore components, Ndc10, Cep3, and Mif2. Still images were taken after rapamycin addition for 3 h at 27°C, a permissive temperature for all mutants. I scored unsegregated GFP dots in large-budded cells that had separated the Spc42-mCherry signals in mother and bud and an abnormal number of GFP dots (0 or 2) in cells carrying one Spc42-mCherry dot, of which the latter represents chromosome missegregation in previous mitosis (Figure 2C). The fraction of cells with abnormal GFP dots was very low in all LacI cells, except in *ipl1-321*, indicating that segregation of the normal chromosome was only affected in *ipl1-321* at 27°C (Figure 2C). Expression of LacI-FRB caused a marked increase of cells with abnormal GFP dots in the wild type (Figure 2C), consistent with the result obtained by time-lapse analysis. This fraction was increased by more than twofold in all four mitotic mutants compared with the wild type (Figure 2C), indicating that the mutations promote chromosome missegregation. The fraction of cells containing unsegregated GFP dots was also increased in LacI-FRB cells compared with the LacI control, consistent with a delay in chromosome segregation. The difference in this fraction of cells among the wild type and the mutants was marginal, suggesting similar segregation time in anaphase. The results indicate that segregation of the tethered chromosome requires an intact kinetochore–microtubule attachment.

Having established that tethering to the NE impacts the segregation of sister chromatids distal to the tether, I next examined the region proximal to the centromere by inserting *tetO* repeats at 1200 kb in between *CEN4* and the *lacO* insert (Figure 3A). Time-lapse imaging showed that more than 90% of LacI-FRB cells (n = 43) successfully segregated the 1200 kb locus during anaphase, even though the segregation time and the spindle length at segregation were still longer than in the LacI cells (Figure 3A). The GFP dots failed to closely follow the SPBs during late anaphase and were not separated to the same extent as in the LacI control cells (Figure 3A). Therefore, chromosome tethering to the NE also affects the dynamic movement of the region proximal to the centromere.

I next inserted the *tetO* repeat at the *TRP1* locus, ~12 kb from *CEN4*. Time-lapse imaging showed successful segregation in all cells expressing either LacI (n = 24) or LacI-FRB (n = 54) (Figure 3B). In both cells, the GFP dot split shortly after anaphase onset and closely followed the separating SPBs (Figure 3B). However, in almost all LacI-FRB cells, one or both of the GFP dots transiently dissociated from the SPB during anaphase, showing oscillation of the distance between the separating GFP dots (Figure 3B). Thus, the chromosome tether even impacts the movement of the centromere >1000 kb away.

The SPBs snapped back at the end of anaphase in some of the chromosome-tethered cells (Figures 2A and 3A). This phenotype was observed with the tether at 37 kb of ChrIV near the left telomere (unpublished data), at 1475 kb or at both loci. Time-lapse imaging of GFP-Tub1 showed that the mitotic spindle broke at the midzone immediately before the pole–pole distance shortened in control cells (Figure 4A, left). In cells with double tethers, spindle collapse usually occurred after breakage, while some cells showed spindle

segregated chromatin marked by tetR-GFP is shown in the table. (C) Effect of mitotic mutations on the segregation of the tethered chromosome. Maximum-intensity projection image of tetR-GFP targeted to 1500 kb of ChrIV with the tether at 1475 kb. White arrowheads, no GFP dot; yellow arrowhead, unsegregated GFP dot. Scale bar: 4 μm. Cells were scored for unsegregated or abnormal number of tetR-GFP. The graph shows mean value and SD from four experiments with more than 250 cells for each sample.

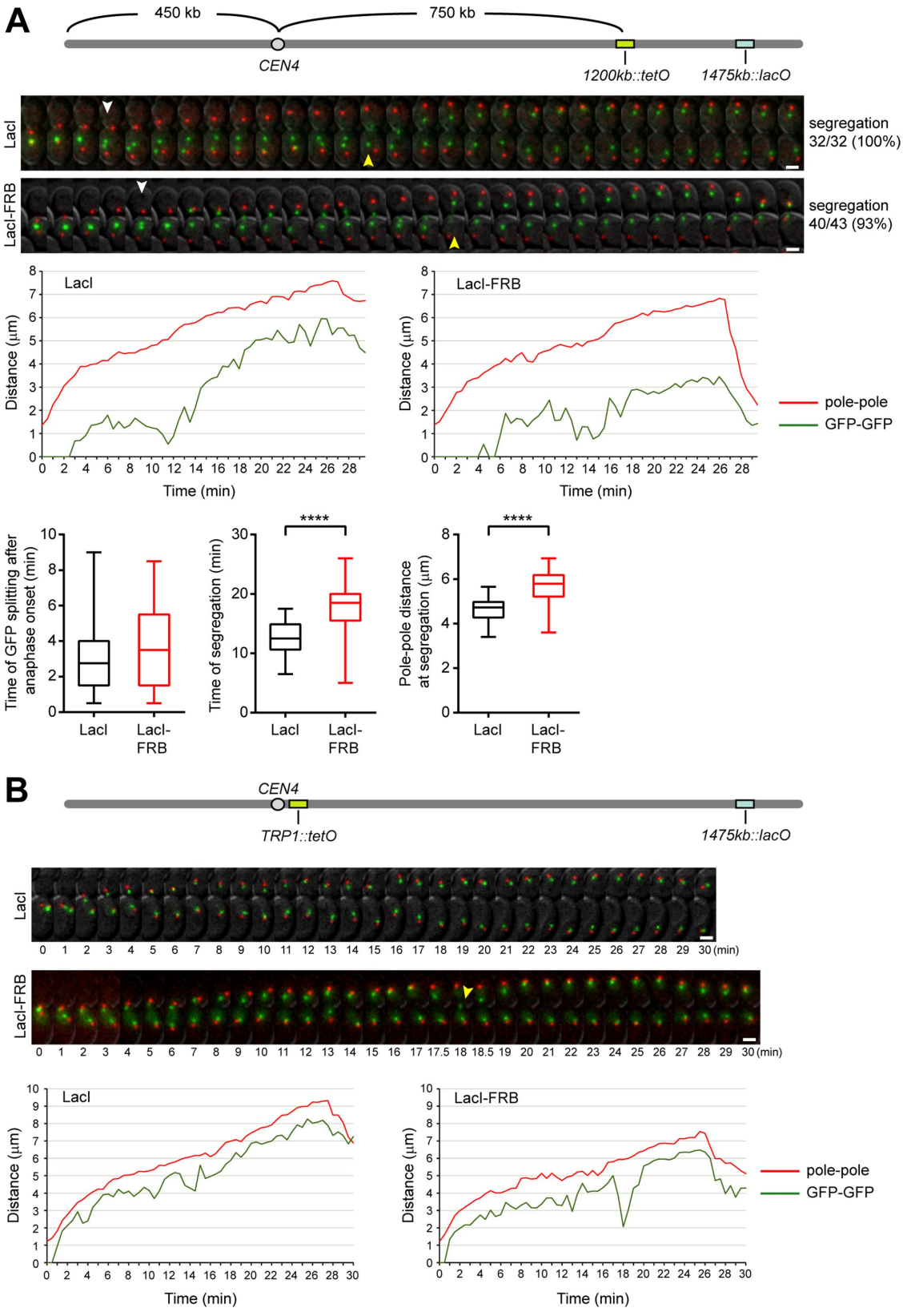

FIGURE 3: Effect of chromosome–NE tethering on centromere-proximal region. (A) Time-lapse images of cells with *tetO* and *lacO* inserted at 1200 and 1475 kb, respectively. Maximum-intensity projection images with 1-min intervals are shown. White and yellow arrowheads indicate sister chromatid splitting and segregation, respectively. Measurements from the time series are plotted. Two-tailed unpaired Student's *t* test, ****, $p < 0.0001$. (B) Time-lapse images of cells with *tetO* and *lacO* inserted at the *TRP1* locus near *CEN4* and 1475 kb, respectively (also see Supplemental Video 2). The time after anaphase onset is shown below the images. Yellow arrowhead indicates dissociation of a GFP dot from the SPB. Measurements from the time series are plotted.

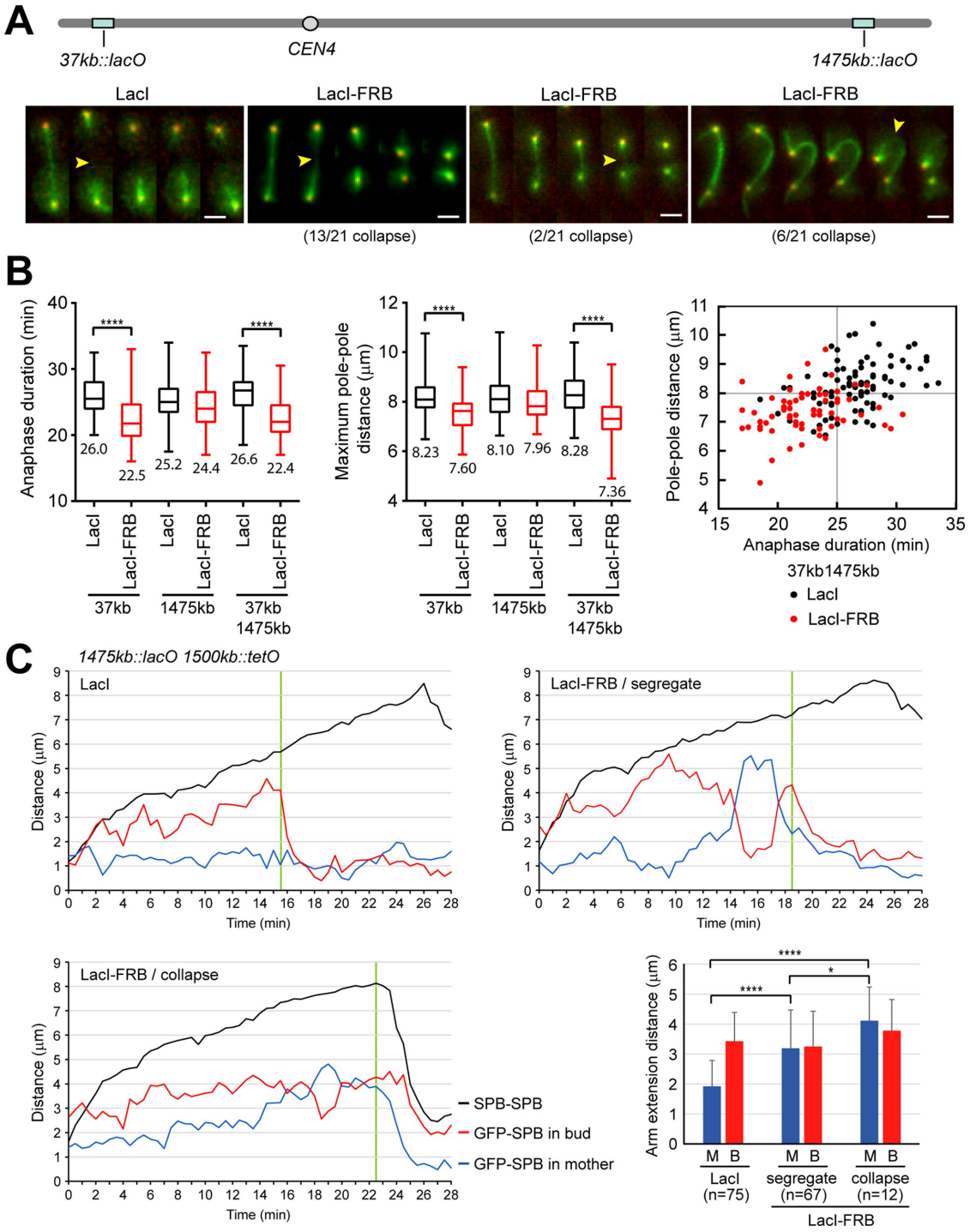

FIGURE 4: Effect of chromosome–NE tethering on spindle and chromosome extension. (A) Time-lapse images of GFP-Tub1 in cells with *lacO* inserts at 37 and 1475 kb. Maximum-intensity projection images of late anaphase cells with 1-min intervals are shown (also see Supplemental Video 3). The fraction of three types of collapsed spindle is indicated. SPBs are marked with Spc42-mCherry. Yellow arrowheads indicate breaks at the spindle midzone. Scale bar: 2 μm. (B) Measurements from time series of cells with *lacO* inserts at 37 kb ($n = 83$ for LacI, $n = 71$ for LacI-FRB), 1475 kb ($n = 80$ for LacI, $n = 88$ for LacI-FRB), or both loci ($n = 87$ for LacI, $n = 69$ for LacI-FRB). The average is shown below the lower whisker. Two-tailed unpaired Student's *t* test, ****, $p < 0.0001$. Comparison of maximum pole–pole distance and anaphase duration in cells with double tethers at 37 and 1475 kb is shown on the right. Each dot represents one cell. (C) The distance between tetR-GFP and the proximal SPB in the mother or bud was measured during anaphase in *1475kb::lacO 1500kb::tetO* cells. The distance at the time when the GFP dots started to segregate, as indicated by the green line, was used as the chromosome arm extension distance in the plot. For LacI-FRB cells with collapsed SPBs, the time point before collapse was used. M, mother; B, bud. Two-tailed unpaired Student's *t* test, ****, $p < 0.0001$; *, $p < 0.05$.

contraction or bending toward the bud neck, forming a hooklike structure before breakage (Figure 4A). Similar results were also found with a single tether (unpublished data). Thus, the force generated from chromosome–NE tethering not only opposes spindle extension, but also causes spindle bending or shrinkage.

I compared the effect of a single tether at either or both ends of ChrIV. Both the anaphase duration and maximum pole–pole distance were slightly reduced with the tether at 1475 kb in comparison with the control (Figures 2A and 4B). They were significantly reduced with the tether at 37 kb and with double tethers at 37 and 1475 kb compared with the control (Figure 4B). The parallel reduction of anaphase duration and the maximum pole–pole distance was apparent in cells with double tethers compared with the control (Figure 4B). Thus, the effect of tethering was more pronounced with the tether on a short chromosome arm than on a long arm and was further enhanced with tethers at both ends of the chromosome.

Stretching of tethered chromosome might limit spindle elongation. Indeed, the chromosome arm extension distance before sister segregation, as measured by the distance between tetR-GFP and the proximal SPB, showed that tethering at 1475 kb caused a 1.7-fold increase in the length in the mother side of the cell that segregated the locus, in comparison with the LacI control. In cells with a collapsed spindle, the length increased to 2.1-fold in the mother and slightly increased in the bud (Figure 4C). The measurements also reflected the back-and-forth oscillation of the tethered chromosome (Figure 2A). The data support that tethering to the NE causes chromosome overstretching and limits spindle extension. Similar phenotypes have previously been found in cells carrying a dicentric chromosome, with counteracting force generated from centromeres attached to the opposite SPBs (Thrower and Bloom, 2001).

In summary, I used the conditional and versatile chromosome-tethering system to study how tethering a defined chromosome locus to the NE affects the anaphase dynamics of different regions of the chromosome and the spindle. With a fully functional mitotic apparatus, the mitotic force from the spindle could physically dislodge the tether from the NE or move the tethered chromosome along the NE to segregate the sisters (Figure 5). The region distal to the tether, but not proximal to the centromere, is occasionally missegregated, likely as a result of chromosome breakage caused by chromosome overstretching during anaphase or severing of the unsegregated chromosome during cytokinesis (Figure 5), similar to previous findings with a dicentric chromosome (Thrower and Bloom, 2001; Lopez *et al.*, 2015). Tension from chromosome stretching could stimulate the growth of kinetochore microtubules and move the chromosome toward the cell center. Alternate stretching and recoiling of the tethered chromosome could produce oscillation between the mother and bud, as observed in time-lapse imaging (Figures 2 and 3). Chromosome recoiling without the growth of kinetochore microtubules could result in shortening or bending of the spindle (Figures 4A and 5). This study supports that chromosomes must dissociate from the NE to move freely and to segregate in closed mitosis, as in open mitosis.

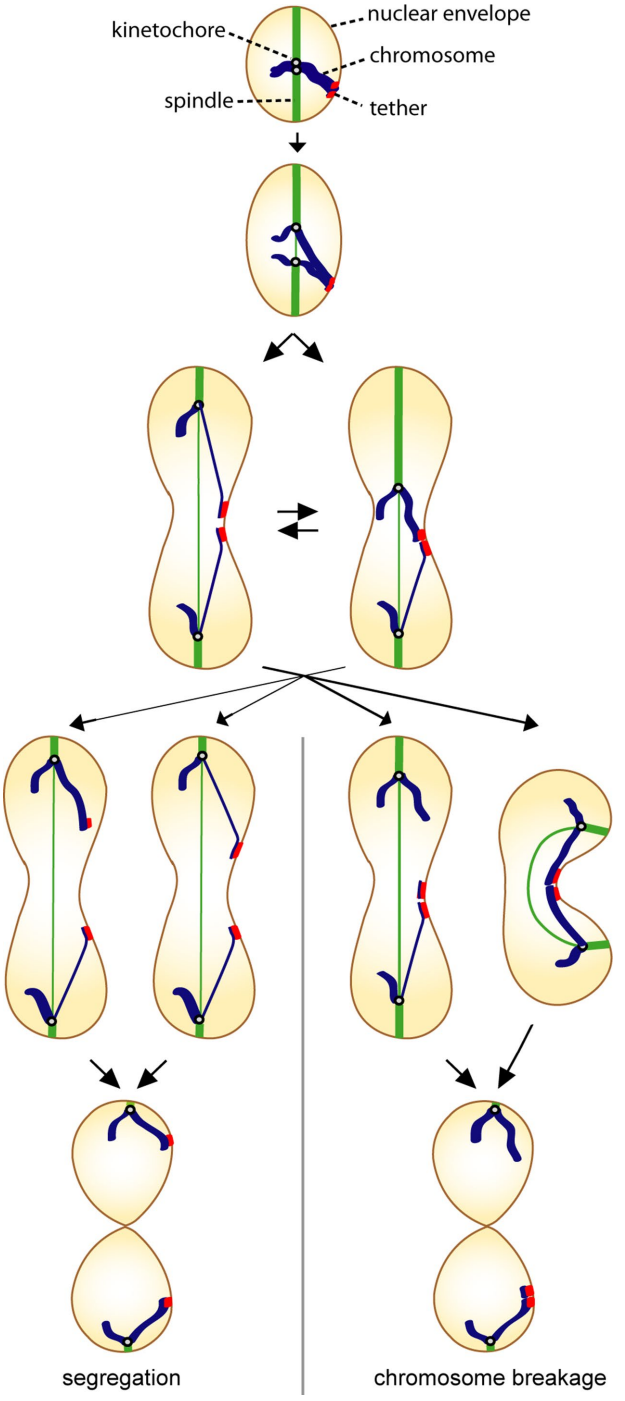

FIGURE 5: Model for the consequence of chromosome–NE tethering. The tethered chromosome oscillates between stretching and recoiling during anaphase. The tension from overstretching dislodges the tether or pulls the tethered chromosome along the NE, leading to chromosome segregation. Alternatively, the overstretched chromosome breaks between the centromere and the tether during anaphase or cytokinesis. Recoiling of both sister chromatids causes spindle bending or shortening, followed by cytokinesis and chromatin severing.

MATERIALS AND METHODS

Plasmids

For expressing LacI in yeast cells, I constructed plasmid pRC2619 containing the *HIS3* promoter at *Sac*I-*Not*I, LacI along with the C-terminal nuclear localization sequence (NLS) amplified by PCR from pAFS135 (Straight *et al.*, 1998) at *Spe*I-*Eco*RI, and the *CYC1* terminator at *Xho*I-*Kpn*I in pRS403. For LacI-FRB expression, the FRB sequence was amplified from pFA6a-FRB-GFP-KanMX6 (Haruki *et al.*, 2008) (from EUROSCARF) and inserted between LacI and NLS at *Bam*HI in pRC2619 to generate pRC2620. These plasmids were linearized with *Pst*I for integration at the *HIS3* locus. The protein expression was confirmed by Western blot with anti-LacI antibody

(Abcam, Cambridge, UK). For expressing tetR-GFP, the *URA3* promoter was cloned at *Not*I, tetR with the N-terminal NLS from plasmid 3524 (Michaelis *et al*., 1997) was cloned at *Bam*HI-*Xma*I, dimerization-deficient GFP (A206K) was cloned at *Cla*I-*Sal*I, and *CYC1* terminator was cloned at *Xho*I-*Kpn*I in pRS405. The resulting plasmid, pRC2571, was linearized with *Afl*II to integrate at the *LEU2* locus, and protein expression was examined by fluorescence microscopy.

For *lacO* integration constructs, the *URA3* gene between *Aat*II-*Nae*I in pRS406 was replaced by a *loxP-KanMX6-loxP* cassette amplified by PCR from pUG6 (Gueldener *et al*., 2002). The *lacOx256* sequence from pAFS52 (Straight *et al*., 1996) was subcloned at *Bam*HI-*Hin*dIII, and DNA sequences corresponding to various regions of ChrIV were amplified by PCR from genomic DNA and individually cloned at *Not*I-*Bam*HI. The resulting plasmids, pRC2503 and pRC2511, were linearized with *Bst*BI to integrate in the *MFG1* gene at ~37 kb and in the upstream region of *AHA1* at ~900 kb of ChrIV, respectively. pRC2507 was linearized with *Pme*I to integrate in the upstream region of *SLF1* at ~1475 kb. The integration was determined by colony PCR of yeast transformants, and the cells were subsequently crossed to a strain expressing LacI-GFP to confirm the GFP dot by fluorescence microscopy.

For *tetO* integration constructs, *tetOx112* was cloned at *Bam*HI-*Hin*dIII, and various regions of ChrIV were amplified by PCR from genomic DNA at *Bam*HI-*Not*I. For integration at ~1200 kb, the construct (pRC2596) was made in pRS404 and linearized with *Bst*BI to integrate in the promoter region of *ESC2*. For integration at other loci, the constructs were made in pRS406. pRC2598 was linearized with *Pme*I for integration in the promoter region of *FIT1* at ~1500 kb. pRC2629 was linearized with *Sna*BI for integration in the promoter region of *TRP1* near *CEN4*. pRC2649 was linearized with *Afl*II for integration in *YDR246W-A* at ~950 kb. The integration was confirmed by colony PCR of yeast transformants.

For expressing GFP-Tub1, I constructed a plasmid containing *CYC1* promoter at *Sac*I-*Xba*I, *GFP* at *Xba*I-*Bam*HI, *TUB1* coding sequence at *Bam*HI-*Sal*I, in-frame with *GFP*, and *CYC1* terminator at *Xho*I-*Kpn*I in pRS403. The plasmid was linearized with *Nhe*I for integration at *HIS3* locus.

Yeast strains

All experiments were performed with diploid yeast. Both *MATa* and *MATα* cells carried *tor1-1* and were deleted for *FPR1*, the major rapamycin acceptor, to confer resistance to rapamycin. Except for the experiment shown in Figure 2B, *lacO* and *tetO* repeats were inserted into *MATa* cells, while *MATα* cells expressed LacI or LacI-FRB and TetR-GFP. For studying the effect of the chromosome tether in *trans* shown in Figure 2B, *lacO* was inserted at ~1475 kb of ChrIV in *MATa*, while *tetO* was inserted at ~1500 kb of ChrIV in *MATα*. *MATa* cells also expressed Src1-2xFKBP12 that was generated by one-step PCR-mediated gene modification using pFA6a-2xFKBP12-loxP-TRP1-loxP (from EUROSCARF) as the PCR template. The expression was confirmed by Western blot with anti-mTOR antibody (Enzo Life Sciences, Farmingdale, NY). *TRP1* marker was subsequently removed by the expression of Cre recombinase from pSH47 in some cells, as indicated in the strain list (Supplemental Table S1) (Gueldener *et al*., 2002). Spc42-mCherry and Nup2-mCherry were generated by one-step PCR-mediated gene modification (Longtine *et al*., 1998), and confirmed by fluorescence microscopy. *MATa* and *MATα* cells were mated to produce diploid cells of the desired genotypes. Experiments were performed with either freshly mated diploid cells or with cells inoculated from the frozen stock for less than 1 wk, to avoid any adverse effect from the basal level of chromosome tethering. For experiments with temperature-sensitive mutants, *tor1-1 fpr1Δ* cells were crossed to mutants of the other mating type; this was followed by sporulation and tetrad analysis. Temperature-sensitive cells carrying *tor1-1 fpr1Δ* were selected for further genetic modification as described earlier.

Image acquisition and processing

All images were acquired with a DeltaVision system (GE Healthcare Life Sciences, Pittsburgh, PA). Still images shown in Figure 1 were taken using a PlanApo N 60×/NA 1.42 oil lens (Olympus, Tokyo, Japan) and sCMOS camera (pco.edge 4.2; PCO AG, Kelheim, Germany). Still images used in Figure 2C and all time-lapse images were taken with a UPlanSApo 100×/NA 1.4 oil lens (Olympus, Tokyo, Japan) and an EMCCD camera (Evolve 512; Photometrics, Tucson, AZ). For the still images shown in Figure 2C, cells were first grown at 25°C to early log phase and then treated with 10 μg/ml rapamycin (Sigma, St. Louis, MO) for 3 h at 27°C. For time-lapse imaging, cells were grown to log phase at 30°C and then treated with 10 μg/ml rapamycin for 10 min at room temperature. Cells were concentrated by centrifugation and spotted onto a layer of 2% agarose made in synthetic complete medium. The coverslip was sealed on the slide with Vaseline/lanolin/paraffin wax in equal parts. The images were taken in a microscope chamber set at 27°C. z-Stacks of eight optical sections with spacing of 0.4 μm (for results in Figure 1) or 12 optical sections with spacing of 0.5 μm (for all other experiments) were collected and processed by Softworx software (Version 7.0.0; GE Healthcare Life Sciences, Pittsburgh, PA). The measurements of time and distance in the images were performed with ImageJ software (https://imagej.nih.gov/ij). Distance was measured on the maximum-intensity projection images using Straight Line and measurement tools in ImageJ. The distance between the tetR-GFP dot and the NE marked by Nup2-mCherry was measured from a single focal plane of z-stack images. Only the GFP signal near the midzone of the cell was used for clarity, as previously reported (Fujita *et al*., 2012). The data sets were exported into Microsoft Excel (Microsoft Office 2013; Microsoft, Richmond, WA) and GraphPad Prism (Version 8.0.0; GraphPad Software, San Diego, CA) for statistical analysis.

ACKNOWLEDGMENTS

The work was supported by grants from the Minister of Science and Technology, Taiwan (MOST 106-2311-B-001-012-MY3), and Academia Sinica.

REFERENCES

Champion L, Linder MI, Kutay U (2017). Cellular reorganization during mitotic entry. Trends Cell Biol 27, 26–41.

Champion L, Pawar S, Luithle N, Ungricht R, Kutay U (2019). Dissociation of membrane-chromatin contacts is required for proper chromosome segregation in mitosis. Mol Biol Cell 30, 427–440.

Chikashige Y, Yamane M, Okamasa K, Tsutsumi C, Kojidani T, Sato M, Haraguchi T, Hiraoka Y (2009). Membrane proteins Bqt3 and -4 anchor telomeres to the nuclear envelope to ensure chromosomal bouquet formation. J Cell Biol 187, 413–427.

Foisner R, Gerace L (1993). Integral membrane proteins of the nuclear envelope interact with lamins and chromosomes, and binding is modulated by mitotic phosphorylation. Cell 73, 1267–1279.

Fujita I, Nishihara Y, Tanaka M, Tsujii H, Chikashige Y, Watanabe Y, Saito M, Ishikawa F, Hiraoka Y, Kanoh J (2012). Telomere-nuclear envelope dissociation promoted by Rap1 phosphorylation ensures faithful chromosome segregation. Curr Biol 22, 1932–1937.

Gueldener U, Heinisch J, Koehler GJ, Voss D, Hegemann JH (2002). A second set of loxP marker cassettes for Cre-mediated multiple gene knockouts in budding yeast. Nucleic Acids Res 30, e23.

Haruki H, Nishikawa J, Laemmli UK (2008). The anchor-away technique: rapid, conditional establishment of yeast mutant phenotypes. Mol Cell 31, 925–932.

Heald R, McKeon F (1990). Mutations of phosphorylation sites in lamin A that prevent nuclear lamina disassembly in mitosis. Cell 61, 579–589.
Hediger F, Neumann FR, Van Houwe G, Dubrana K, Gasser SM (2002). Live imaging of telomeres: yKu and Sir proteins define redundant telomere-anchoring pathways in yeast. Curr Biol 12, 2076–2089.
Hirano Y, Iwase Y, Ishii K, Kumeta M, Horigome T, Takeyasu K (2009). Cell cycle-dependent phosphorylation of MAN1. Biochemistry 48, 1636–1643.
Hirano Y, Segawa M, Ouchi FS, Yamakawa Y, Furukawa K, Takeyasu K, Horigome T (2005). Dissociation of emerin from barrier-to-autointegration factor is regulated through mitotic phosphorylation of emerin in a *Xenopus* egg cell-free system. J Biol Chem 280, 39925–39933.
Laroche T, Martin SG, Gotta M, Gorham HC, Pryde FE, Louis EJ, Gasser SM (1998). Mutation of yeast Ku genes disrupts the subnuclear organization of telomeres. Curr Biol 8, 653–656.
Laroche T, Martin SG, Tsai-Pflugfelder M, Gasser SM (2000). The dynamics of yeast telomeres and silencing proteins through the cell cycle. J Struct Biol 129, 159–174.
Longtine MS, McKenzie A 3rd, Demarini DJ, Shah NG, Wach A, Brachat A, Philippsen P, Pringle JR (1998). Additional modules for versatile and economical PCR-based gene deletion and modification in *Saccharomyces cerevisiae*. Yeast 14, 953–961.
Lopez V, Barinova N, Onishi M, Pobiega S, Pringle JR, Dubrana K, Marcand S (2015). Cytokinesis breaks dicentric chromosomes preferentially at pericentromeric regions and telomere fusions. Genes Dev 29, 322–336.
Michaelis C, Ciosk R, Nasmyth K (1997). Cohesins: chromosomal proteins that prevent premature separation of sister chromatids. Cell 91, 35–45.
Molitor TP, Traktman P (2014). Depletion of the protein kinase VRK1 disrupts nuclear envelope morphology and leads to BAF retention on mitotic chromosomes. Mol Biol Cell 25, 891–903.
Nichols RJ, Wiebe MS, Traktman P (2006). The vaccinia-related kinases phosphorylate the N′ terminus of BAF, regulating its interaction with DNA and its retention in the nucleus. Mol Biol Cell 17, 2451–2464.
Stern BM (2002). Mitosis: aurora gives chromosomes a healthy stretch. Curr Biol 12, R316–R318.
Straight AF, Belmont AS, Robinett CC, Murray AW (1996). GFP tagging of budding yeast chromosomes reveals that protein-protein interactions can mediate sister chromatid cohesion. Curr Biol 6, 1599–1608.
Straight AF, Sedat JW, Murray AW (1998). Time-lapse microscopy reveals unique roles for kinesins during anaphase in budding yeast. J Cell Biol 143, 687–694.
Taddei A, Gasser SM (2004). Multiple pathways for telomere tethering: functional implications of subnuclear position for heterochromatin formation. Biochim Biophys Acta 1677, 120–128.
Taddei A, Hediger F, Neumann FR, Bauer C, Gasser SM (2004). Separation of silencing from perinuclear anchoring functions in yeast Ku80, Sir4 and Esc1 proteins. EMBO J 23, 1301–1312.
Thrower DA, Bloom K (2001). Dicentric chromosome stretching during anaphase reveals roles of Sir2/Ku in chromatin compaction in budding yeast. Mol Biol Cell 12, 2800–2812.
Titos I, Ivanova T, Mendoza M (2014). Chromosome length and perinuclear attachment constrain resolution of DNA intertwines. J Cell Biol 206, 719–733.
Tseng LC, Chen RH (2011). Temporal control of nuclear envelope assembly by phosphorylation of lamin B receptor. Mol Biol Cell 22, 3306–3317.